

**Web-based Supplementary Materials for A Space-time Skew- $t$  Model for Threshold  
Exceedances by Morris, Reich, Thibaud, and Cooley**

**Samuel A Morris<sup>1,\*</sup>, Brian J Reich<sup>1</sup>, Emeric Thibaud<sup>2</sup>, and Daniel Cooley<sup>2</sup>**

<sup>1</sup>Department of Statistics, North Carolina State University, Raleigh, North Carolina, U.S.A.

<sup>2</sup>Department of Statistics, Colorado State University, Fort Collins, Colorado, U.S.A.

*\*email:* samorris@ncsu.edu

## Web Appendix A. MCMC details

The MCMC sampling for the model in Section 4 is done using R (<http://www.r-project.org>). Whenever possible, we select conjugate priors (see Web Appendix B); however, for some of the parameters, no conjugate prior distributions exist. For these parameters, we use a random walk Metropolis-Hastings update step. In each Metropolis-Hastings update, we tune the algorithm during the burn-in period to give acceptance rates near 0.40.

### *Spatial knot locations*

For each day, we update the spatial knot locations,  $\mathbf{w}_1, \dots, \mathbf{w}_K$ , using a Metropolis-Hastings block update. Because the spatial domain is bounded, we generate candidate knots using the transformed knots  $\mathbf{w}_1^*, \dots, \mathbf{w}_K^*$  (see Section 3.3) and a random walk bivariate Gaussian candidate distribution

$$\mathbf{w}_k^{*(c)} \sim N(\mathbf{w}_k^{*(r-1)}, s^2 I_2)$$

where  $\mathbf{w}_k^{*(r-1)}$  is the location for the transformed knot at MCMC iteration  $r - 1$ ,  $s$  is a tuning parameter, and  $I_2$  is an identity matrix. Let  $\mathbf{Y}_t = [Y(\mathbf{s}_1), \dots, Y(\mathbf{s}_n)]$  be the vector of observed responses at each site for day  $t$ . After candidates have been generated for all  $K$  knots, the acceptance ratio is

$$R = \left\{ \frac{l[\mathbf{Y}_t | \mathbf{w}_1^{(c)}, \dots, \mathbf{w}_K^{(c)}, \dots]}{l[\mathbf{Y}_t | \mathbf{w}_1^{(r-1)}, \dots, \mathbf{w}_K^{(r-1)}, \dots]} \right\} \times \left\{ \frac{\prod_{k=1}^K \phi(\mathbf{w}_k^{(c)})}{\prod_{k=1}^K \phi(\mathbf{w}_k^{(r-1)})} \right\} \times \left\{ \frac{\prod_{k=1}^K p(\mathbf{w}_k^{*(c)})}{\prod_{k=1}^K p(\mathbf{w}_k^{*(r-1)})} \right\}$$

where  $l$  is the likelihood given in (17), and  $p(\cdot)$  is the prior either taken from the time series (see Section 3.3) or assumed to be uniform over  $\mathcal{D}$ . The candidate knots are accepted with probability  $\min\{R, 1\}$ .

### *Spatial random effects*

If there is no temporal dependence amongst the observations, we use a Gibbs update for  $z_{tk}$ , and the posterior distribution is given in Web Appendix B. If there is temporal dependence amongst the observations, then we update  $z_{tk}$  using a Metropolis-Hastings update. Because this model uses

$|z_{tk}|$ , we generate candidate random effects using the  $z_{tk}^*$  (see Section 3.3) and a random walk Gaussian candidate distribution

$$z_{tk}^{*(c)} \sim \mathbf{N}(z_{tk}^{*(r-1)}, s^2)$$

where  $z_{tk}^{*(r-1)}$  is the value at MCMC iteration  $r - 1$ , and  $s$  is a tuning parameter. The acceptance ratio is

$$R = \left\{ \frac{l[\mathbf{Y}_t | z_{tk}^{(c)}, \dots]}{l[\mathbf{Y}_t | z_{tk}^{(r-1)}]} \right\} \times \left\{ \frac{p[z_{tk}^{(c)}]}{p[z_{tk}^{(r-1)}]} \right\}$$

where  $p[\cdot]$  is the prior taken from the time series given in Section 3.3. The candidate is accepted with probability  $\min\{R, 1\}$ .

#### *Variance terms*

When there is more than one site in a partition, then we update  $\sigma_{tk}^2$  using a Metropolis-Hastings update. First, we generate a candidate for  $\sigma_{tk}^2$  using an  $\text{IG}(a^*/s, b^*/s)$  candidate distribution in an independence Metropolis-Hastings update where  $a^* = (n_{tk} + 1)/2 + a$ ,  $b^* = [\mathbf{Y}_{tk}^\top \Sigma_{tk}^{-1} \mathbf{Y}_{tk} + z_{tk}^2]/2 + b$ ,  $n_{tk}$  is the number of sites in partition  $k$  on day  $t$ , and  $\mathbf{Y}_{tk}$  and  $\Sigma_{tk}^{-1}$  are the observations and precision matrix for partition  $k$  on day  $t$ . The acceptance ratio is

$$R = \left\{ \frac{l[\mathbf{Y}_t | \sigma_{tk}^{2(c)}, \dots]}{l[\mathbf{Y}_t | \sigma_{tk}^{2(r-1)}]} \right\} \times \left\{ \frac{l[z_{tk} | \sigma_{tk}^{2(c)}, \dots]}{l[z_{tk} | \sigma_{tk}^{2(r-1)}, \dots]} \right\} \times \left\{ \frac{p[\sigma_{tk}^{2(c)}]}{p[\sigma_{tk}^{2(r-1)}]} \right\} \times \left\{ \frac{c[\sigma_{tk}^{2(r-1)}]}{c[\sigma_{tk}^{2(c)}]} \right\}$$

where  $p[\cdot]$  is the prior either taken from the time series given in Section 3.3 or assumed to be  $\text{IG}(a, b)$ , and  $c[\cdot]$  is the candidate distribution. The candidate is accepted with probability  $\min\{R, 1\}$ .

#### *Spatial covariance parameters*

We update the three spatial covariance parameters,  $\log(\rho)$ ,  $\log(\nu)$ ,  $\gamma$ , using a Metropolis-Hastings block update step. First, we generate a candidate using a random walk Gaussian candidate distribution

$$\log(\rho)^{(c)} \sim \mathbf{N}(\log(\rho)^{(r-1)}, s^2)$$

where  $\log(\rho)^{(r-1)}$  is the value at MCMC iteration  $r - 1$ , and  $s$  is a tuning parameter. Candidates are generated for  $\log(\nu)$  and  $\gamma$  in a similar fashion. The acceptance ratio is

$$R = \left\{ \frac{\prod_{t=1}^{n_t} l[Y_t(\mathbf{s})|\rho^{(c)}, \nu^{(c)}, \gamma^{(c)}, \dots]}{\prod_{t=1}^{n_t} l[Y_t(\mathbf{s})|\rho^{(r-1)}, \nu^{(r-1)}, \gamma^{(r-1)}, \dots]} \right\} \times \left\{ \frac{p[\rho^{(c)}]}{p[\rho^{(r-1)}]} \right\} \times \left\{ \frac{p[\nu^{(c)}]}{p[\nu^{(r-1)}]} \right\} \times \left\{ \frac{p[\gamma^{(c)}]}{p[\gamma^{(r-1)}]} \right\}.$$

All three candidates are accepted with probability  $\min\{R, 1\}$ .

## Web Appendix B. Posterior distributions

*Conditional posterior of  $z_{tk} \mid \dots$*

If knots are independent over days, then the conditional posterior distribution of  $|z_{tk}|$  is conjugate.

For simplicity, drop the subscript  $t$ , let  $\tilde{z}_k = |z_k|$ ,  $\tilde{\mathbf{z}}_{k^c}$  be the vector of  $[|z(\mathbf{s}_1)|, \dots, |z(\mathbf{s}_n)|]$  for  $\mathbf{s} \notin P_k$ ,  $\mathbf{X} = [\mathbf{X}(\mathbf{s}_1), \dots, \mathbf{X}(\mathbf{s}_n)]^\top$ , let  $\mathbf{Y}_k$  and  $\mathbf{X}_k$  be the observations and covariate measurements for  $\mathbf{s} \in P_k$ , and let  $\mathbf{Y}_{k^c}$  and  $\mathbf{X}_{k^c}$  be the observations and covariate measurements for  $\mathbf{s} \notin P_k$  and define

$$\mathbf{R} = \begin{cases} \mathbf{Y}_k - \mathbf{X}_k \boldsymbol{\beta} & \mathbf{s} \in P_k \\ \mathbf{Y}_{k^c} - \mathbf{X}_{k^c} \boldsymbol{\beta} - \lambda \tilde{\mathbf{z}}_{k^c} & \mathbf{s} \notin P_k \end{cases}$$

Let

$\mathbf{R}_1 =$  the vector of  $\mathbf{R}$  for  $\mathbf{s} \in P_k$

$\mathbf{R}_2 =$  the vector of  $\mathbf{R}$  for  $\mathbf{s} \notin P_k$

$$\Omega = \Sigma^{-1}.$$

Then

$$\begin{aligned} \pi(z_k \mid \dots) &\propto \exp \left\{ -\frac{1}{2} \left[ \begin{pmatrix} \mathbf{R}_1 - \lambda \tilde{z}_k \mathbf{1} \\ \mathbf{R}_2 \end{pmatrix}^\top \begin{pmatrix} \Omega_{11} & \Omega_{12} \\ \Omega_{21} & \Omega_{22} \end{pmatrix} \begin{pmatrix} \mathbf{R}_1 - \lambda \tilde{z}_k \mathbf{1} \\ \mathbf{R}_2 \end{pmatrix} + \frac{\tilde{z}_k^2}{\sigma_k^2} \right] \right\} I(z_k > 0) \\ &\propto \exp \left\{ -\frac{1}{2} [\Lambda_k \tilde{z}_k^2 - 2\mu_k \tilde{z}_k] \right\} \end{aligned}$$

where

$$\begin{aligned}\mu_k &= \lambda(\mathbf{R}_1^\top \Omega_{11} + \mathbf{R}_2^\top \Omega_{21})\mathbf{1} \\ \Lambda_k &= \lambda^2 \mathbf{1}^\top \Omega_{11} \mathbf{1} + \frac{1}{\sigma_k^2}.\end{aligned}$$

Then  $\tilde{z}_k | \dots \sim N_{(0,\infty)}(\Lambda_k^{-1} \mu_k, \Lambda_k^{-1})$

*Conditional posterior of  $\beta, \lambda | \dots$*

For models that do not include a skewness parameter, we update  $\beta$  as follows. Let  $\beta \sim \mathbf{N}_p(0, \Lambda_0)$

where  $\Lambda_0$  is a precision matrix. Then

$$\begin{aligned}\pi(\beta | \dots) &\propto \exp \left\{ -\frac{1}{2} \beta^\top \Lambda_0 \beta - \frac{1}{2} \sum_{t=1}^{n_t} [\mathbf{Y}_t - \mathbf{X}_t \beta]^\top \Omega [\mathbf{Y}_t - \mathbf{X}_t \beta] \right\} \\ &\propto \exp \left\{ -\frac{1}{2} \left[ \beta^\top \Lambda_\beta \beta - 2 \sum_{t=1}^{n_t} (\beta^\top \mathbf{X}_t^\top \Omega \mathbf{Y}_t) \right] \right\} \\ &\propto \mathbf{N}(\Lambda_\beta^{-1} \mu_\beta, \Lambda_\beta^{-1})\end{aligned}$$

where

$$\begin{aligned}\mu_\beta &= \sum_{t=1}^{n_t} \mathbf{X}_t^\top \Omega \mathbf{Y}_t \\ \Lambda_\beta &= \Lambda_0 + \sum_{t=1}^{n_t} \mathbf{X}_t^\top \Omega \mathbf{X}_t.\end{aligned}$$

For models that do include a skewness parameter, a simple augmentation of the covariate matrix

$\mathbf{X}$  and parameter vector  $\beta$  allows for a block update of both  $\beta$  and  $\lambda$ . Let  $\mathbf{X}_t^* = [\mathbf{X}_t, |\mathbf{z}_t|]$  where

$\mathbf{z}_t = [z(\mathbf{s}_1), \dots, z(\mathbf{s}_n)]^\top$  and let  $\beta^* = (\beta_1, \dots, \beta_p, \lambda)^\top$ . So to incorporate the  $N(0, \sigma_\lambda^2)$  prior on  $\lambda$ ,

let  $\beta^* \sim \mathbf{N}_{p+1}(0, \Lambda_0^*)$  where

$$\Lambda_0^* = \begin{pmatrix} \Lambda_0 & 0 \\ 0 & \sigma_\lambda^{-2} \end{pmatrix}.$$

Then the update for both  $\beta$  and  $\lambda$  is done using the conjugate prior given above with  $\mathbf{X}_t = \mathbf{X}_t^*$  and

$\beta = \beta^*$

Conditional posterior of  $\sigma^2 \mid \dots$

In the case where  $L = 1$  and temporal dependence is negligible, then  $\sigma^2$  has a conjugate posterior distribution. Let  $\sigma_t^2 \stackrel{iid}{\sim} \text{IG}(\alpha_0/2, \beta_0/2)$ . For simplicity, drop the subscript  $t$ . Then

$$\begin{aligned} \pi(\sigma^2 \mid \dots) &\propto (\sigma^2)^{-\alpha_0/2-1/2-n/2-1} \exp \left\{ -\frac{\beta_0}{2\sigma^2} - \frac{|z|^2}{2\sigma^2} - \frac{(\mathbf{Y} - \boldsymbol{\mu})^\top \Sigma^{-1}(\mathbf{Y} - \boldsymbol{\mu})}{2\sigma^2} \right\} \\ &\propto (\sigma^2)^{-(\alpha_0-1-n)/2-1} \exp \left\{ -\frac{1}{2\sigma^2} [\beta_0 + |z|^2 + (\mathbf{Y} - \boldsymbol{\mu})^\top \Sigma^{-1}(\mathbf{Y} - \boldsymbol{\mu})] \right\} \\ &\propto \text{IG}(\alpha^*, \beta^*) \end{aligned}$$

where

$$\begin{aligned} \alpha^* &= \frac{\alpha_0 + 1 + n}{2} \\ \beta^* &= \frac{1}{2} [\beta_0 + |z|^2 + (\mathbf{Y} - \boldsymbol{\mu})^\top \Sigma^{-1}(\mathbf{Y} - \boldsymbol{\mu})] . \end{aligned}$$

In the case that  $K > 1$ , a random walk Metropolis Hastings step will be used to update  $\sigma_{kt}^2$ .

### Web Appendix C. Proof that $\lim_{h \rightarrow \infty} \pi(h) = 0$

Let  $c$  be the midpoint of  $\mathbf{s}_1$  and  $\mathbf{s}_2$ . Define  $A$  as the circle centered at  $c$  with radius  $h/2$  where  $h = \|\mathbf{s}_1 - \mathbf{s}_2\|$  is the distance between sites  $\mathbf{s}_1$  and  $\mathbf{s}_2$ . Consider a homogeneous spatial Poisson process over  $A$  with intensity  $\lambda_{PP}$ , so that

$$\mu_{PP}(A) = \lambda_{PP}|A| = \lambda_{PP}\pi \left( \frac{h}{2} \right)^2 = \lambda_{PPA}^* h^2.$$

Consider a partition of  $A$  into four regions,  $B_1, B_2, R_1, R_2$  as seen in Web Figure 1.

[Figure 1 about here.]

Let  $N_i$  be the number of knots in  $B_i$  and  $L_i = l$  if  $\mathbf{s}_i \in P_l$  for  $i = 1, 2$ . Then

$$P(L_1 \neq L_2) \geq P(N_1 > 0, N_2 > 0) \quad (1)$$

since knots in both  $B_1$  and  $B_2$  is sufficient, but not necessary, to ensure that  $\mathbf{s}_1$  and  $\mathbf{s}_2$  are in different partition sets. By definition of a Poisson process,  $N_1$  and  $N_2$  are independent and thus

$P(N_1 > 0, N_2 > 0) = P(N_1 > 0)^2$ , and

$$\begin{aligned}\mu_{PP}(B_1) &= \lambda_{PP}|B_1| = \lambda_{PP} \frac{h^2}{4} \left( \frac{2\pi}{3} - \frac{\sqrt{3}}{2} \right) \\ &= \lambda_{PPB_1}^* h^2.\end{aligned}\tag{2}$$

So,

$$P(L_1 \neq L_2) \geq P(N_1 > 0)^2 = [1 - P(N_1 = 0)]^2 = [1 - \exp(-\lambda_{PPB_1}^* h^2)]^2\tag{3}$$

which goes to 1 as  $h$  goes to infinity.

## Web Appendix D. Skew- $t$ distribution

### Univariate skew- $t$ distribution

We say that  $Y$  follows a univariate extended skew- $t$  distribution with location  $\xi \in \mathcal{R}$ , scale  $\omega > 0$ , skew parameter  $\alpha \in \mathcal{R}$ , and degrees of freedom  $\nu$  if has distribution function

$$f_{\text{EST}}(y) = 2f_T(z; \nu)F_T \left[ \alpha z \sqrt{\frac{\nu+1}{\nu+z^2}}; \nu+1 \right]\tag{4}$$

where  $f_T(t; \nu)$  is a univariate Student's  $t$  with  $\nu$  degrees of freedom,  $F_T(t; \nu) = P(T < t)$ , and  $z = (y - \xi)/\omega$ .

### Multivariate skew- $t$ distribution

If  $\mathbf{Z} \sim \text{ST}_d(0, \bar{\boldsymbol{\Omega}}, \boldsymbol{\alpha}, \eta)$  is a  $d$ -dimensional skew- $t$  distribution, and  $\mathbf{Y} = \xi + \boldsymbol{\omega}\mathbf{Z}$ , where  $\boldsymbol{\omega} = \text{diag}(\omega_1, \dots, \omega_d)$ , then the density of  $Y$  at  $y$  is

$$f_y(\mathbf{y}) = \det(\boldsymbol{\omega})^{-1} f_z(\mathbf{z})\tag{5}$$

where

$$f_z(\mathbf{z}) = 2t_d(\mathbf{z}; \bar{\boldsymbol{\Omega}}, \eta) T \left[ \boldsymbol{\alpha}^\top \mathbf{z} \sqrt{\frac{\eta+d}{\nu+Q(\mathbf{z})}}; \eta+d \right]\tag{6}$$

$$\mathbf{z} = \boldsymbol{\omega}^{-1}(\mathbf{y} - \xi)\tag{7}$$

where  $t_d(\mathbf{z}; \bar{\Omega}, \eta)$  is a  $d$ -dimensional Student's  $t$ -distribution with scale matrix  $\bar{\Omega}$  and degrees of freedom  $\eta$ ,  $Q(z) = \mathbf{z}^\top \bar{\Omega}^{-1} \mathbf{z}$  and  $T(\cdot; \eta)$  denotes the univariate Student's  $t$  distribution function with  $\eta$  degrees of freedom (Azzalini and Capitanio, 2014).

### Extremal dependence

For a bivariate skew- $t$  random variable  $\mathbf{Y} = [Y(\mathbf{s}), Y(\mathbf{t})]^\top$ , the  $\chi(h)$  statistic (Padoan, 2011) is given by

$$\chi(h) = \bar{F}_{\text{EST}} \left\{ \frac{[x_1^{1/\eta} - \varrho(h)]\sqrt{\eta+1}}{\sqrt{1 - \varrho(h)^2}}; 0, 1, \alpha_1, \tau_1, \eta + 1 \right\} + \bar{F}_{\text{EST}} \left\{ \frac{[x_2^{1/\eta} - \varrho(h)]\sqrt{\eta+1}}{\sqrt{1 - \varrho(h)^2}}; 0, 1, \alpha_2, \tau_2, \eta + 1 \right\}, \quad (8)$$

where  $\bar{F}_{\text{EST}}$  is the univariate survival extended skew- $t$  function with zero location and unit scale,

$\varrho(h) = \text{cor}[y(\mathbf{s}), y(\mathbf{t})]$ ,  $\alpha_j = \alpha_i \sqrt{1 - \varrho^2}$ ,  $\tau_j = \sqrt{\eta+1}(\alpha_j + \alpha_i \varrho)$ , and  $x_j = F_T(\bar{\alpha}_i \sqrt{\eta+1}; 0, 1, \eta) / F_T(\bar{\alpha}_j \sqrt{\eta+1}; 0, 1, \eta)$  with  $j = 1, 2$  and  $i = 2, 1$  and where  $\bar{\alpha}_j = (\alpha_j + \alpha_i \varrho) / \sqrt{1 + \alpha_i^2 [1 - \varrho(h)^2]}$ .

*Proof that  $\lim_{h \rightarrow \infty} \chi(h) > 0$*

Consider the bivariate distribution of  $\mathbf{Y} = [Y(\mathbf{s}), Y(\mathbf{t})]^\top$ , with  $\varrho(h)$  given by (2). So,  $\lim_{h \rightarrow \infty} \varrho(h) = 0$ . Then

$$\lim_{h \rightarrow \infty} \chi(h) = \bar{F}_{\text{EST}} \left\{ \sqrt{\eta+1}; 0, 1, \alpha_1, \tau_1, \eta + 1 \right\} + \bar{F}_{\text{EST}} \left\{ \sqrt{\eta+1}; 0, 1, \alpha_2, \tau_2, \eta + 1 \right\}. \quad (9)$$

Because the extended skew- $t$  distribution is not bounded above, for all  $\bar{F}_{\text{EST}}(x) = 1 - F_{\text{EST}}(x) > 0$  for all  $x < \infty$ . Therefore, for a skew- $t$  distribution,  $\lim_{h \rightarrow \infty} \chi(h) > 0$ .

## Web Appendix E. Comparisons with other parameterizations

Various forms of multivariate skew-normal and skew- $t$  distributions have been proposed in the literature. In this section, we make a connection between our parameterization in (1) of the main text and another popular version. Azzalini and Capitanio (2014) and Beranger et al. (2016) define



a skew-normal process as

$$\tilde{X}(\mathbf{s}) = \tilde{\lambda}|z| + (1 - \tilde{\lambda}^2)^{1/2}v(\mathbf{s}) \quad (10)$$

where  $\tilde{\lambda} \in (-1, 1)$ ,  $z \sim N(0, 1)$ , and  $v(\mathbf{s})$  is a Gaussian process with mean zero, variance one, and spatial correlation function  $\rho$ . To extend this to the skew- $t$  distribution, Azzalini and Capitanio (2003) take  $\tilde{Y}(\mathbf{s}) = W\tilde{X}(\mathbf{s})$  where  $W^{-2} \sim \text{Gamma}(a/2, a/2)$ . Returning to the proposed parameterization (with  $\beta = 0$ ), let  $W^{-2} = \frac{b}{a}\sigma^{-2}$  so that (1) in the manuscript becomes

$$Y(\mathbf{s}) = W \left[ \lambda \left( \frac{b}{a} \right)^{1/2} |z| + \left( \frac{b}{a} \right)^{1/2} v(\mathbf{s}) \right]. \quad (11)$$

Clearly setting  $b/a = (1 - \tilde{\lambda}^2) > 0$ , and  $\lambda = \tilde{\lambda}/(1 - \tilde{\lambda}^2)^{1/2} \in (-\infty, \infty)$  resolves the difference in parameterizations. We note that our parameterization has three parameters  $(a, b, \lambda)$  compared to the two parameters of the alternative parameterization  $(a, \tilde{\lambda})$ . Since we have assumed that both  $v(\mathbf{s})$  and  $z$  have unit scale, the additional  $b$  parameter in our parameterization is required to control the precision.

## Web Appendix F. Temporal dependence

It is very challenging to derive an analytical expression the temporal extremal dependence at a single site  $\mathbf{s}$ . However, using simulated data, we have evidence to suggest that the model does exhibits temporal extremal dependence. To demonstrate that our model maintains temporal extremal dependence, we generate lag- $m$  observations for  $m = 1, 3, 5, 10$  from our model setting  $\phi_w = \phi_z = \phi_\sigma = \varphi$ , for  $\varphi = 0, 0.02, 0.04, \dots, 1$ . To estimate the lag- $m$  chi-statistic  $\chi(m)$  we first estimate the lag- $m$   $F$ -madogram  $\nu_F(m)$  (Cooley et al., 2006) using  $\hat{\nu}_F(m) = \frac{1}{2n} \sum_{i=1}^n |\hat{F}(y_0) - \hat{F}(y_m)|$  where  $\hat{F}(\cdot)$  represents an empirical CDF and  $y_m$  is the lag- $m$  observation. The  $F$ -madogram is related to the  $\chi$  statistic as follows

$$\chi = 2 - \frac{1 + 2\nu_F}{1 - 2\nu_F}. \quad (12)$$

Web Figure 2 suggests that the extremal dependence increases as  $\varphi \rightarrow 1$ , and that the extremal dependence decreases as  $m$  increases.

[Figure 2 about here.]

### **Web Appendix G. Brier scores for ozone prediction**

Because typical ozone concentration varies throughout the US, we have included Brier scores for exceedance of the 99th quantile by site for two model fits (Gaussian and Symmetric- $t$ ,  $K = 10$  knots,  $T = 75$ , time series) in Web Figure 3. As we can see in these plots, both models seem to perform similarly across the US with the poorest performance in California. Other methods have similar Brier score maps to these.

[Figure 3 about here.]

### **Web Appendix H. Simulation study pairwise difference results**

The following tables show the methods that have significantly different Brier scores when using a Wilcoxon-Nemenyi-McDonald-Thompson test. In each column, different letters signify that the methods have significantly different Brier scores. For example, there is significant evidence to suggest that method 1 and method 4 have different Brier scores at  $q(0.90)$ , whereas there is not significant evidence to suggest that method 1 and method 2 have different Brier scores at  $q(0.90)$ . In each table group A represents the group with the lowest Brier scores. Groups are significant with a familywise error rate of  $\alpha = 0.05$ .

[Table 1 about here.]

[Table 2 about here.]

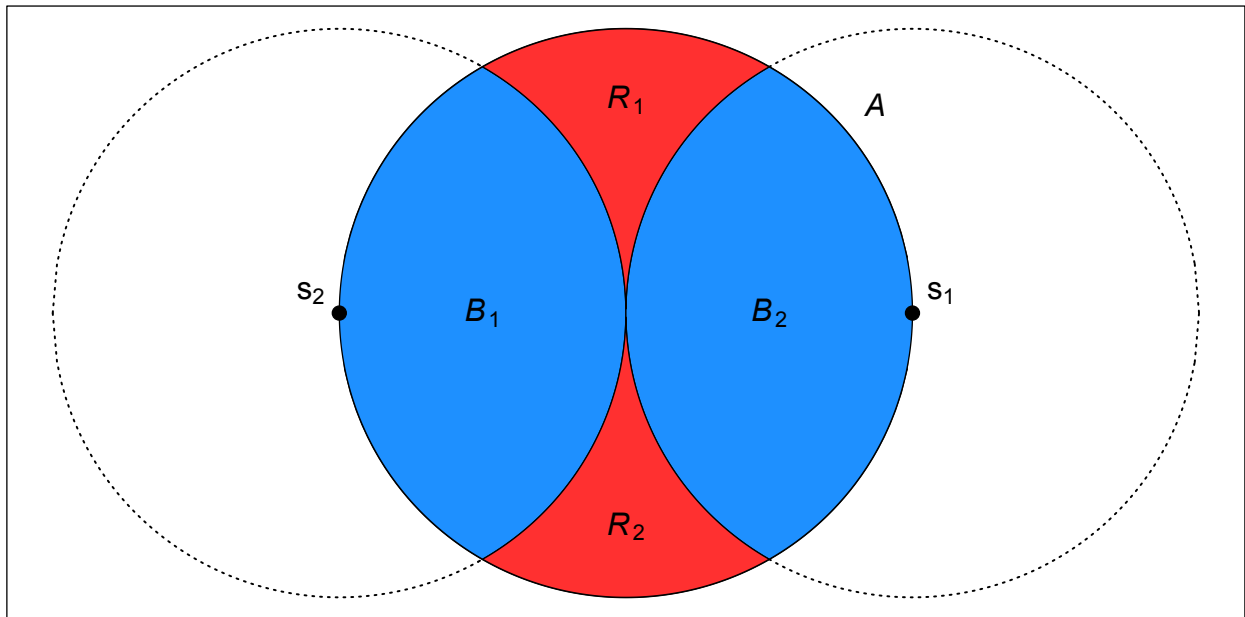
[Table 3 about here.]

[Table 4 about here.]

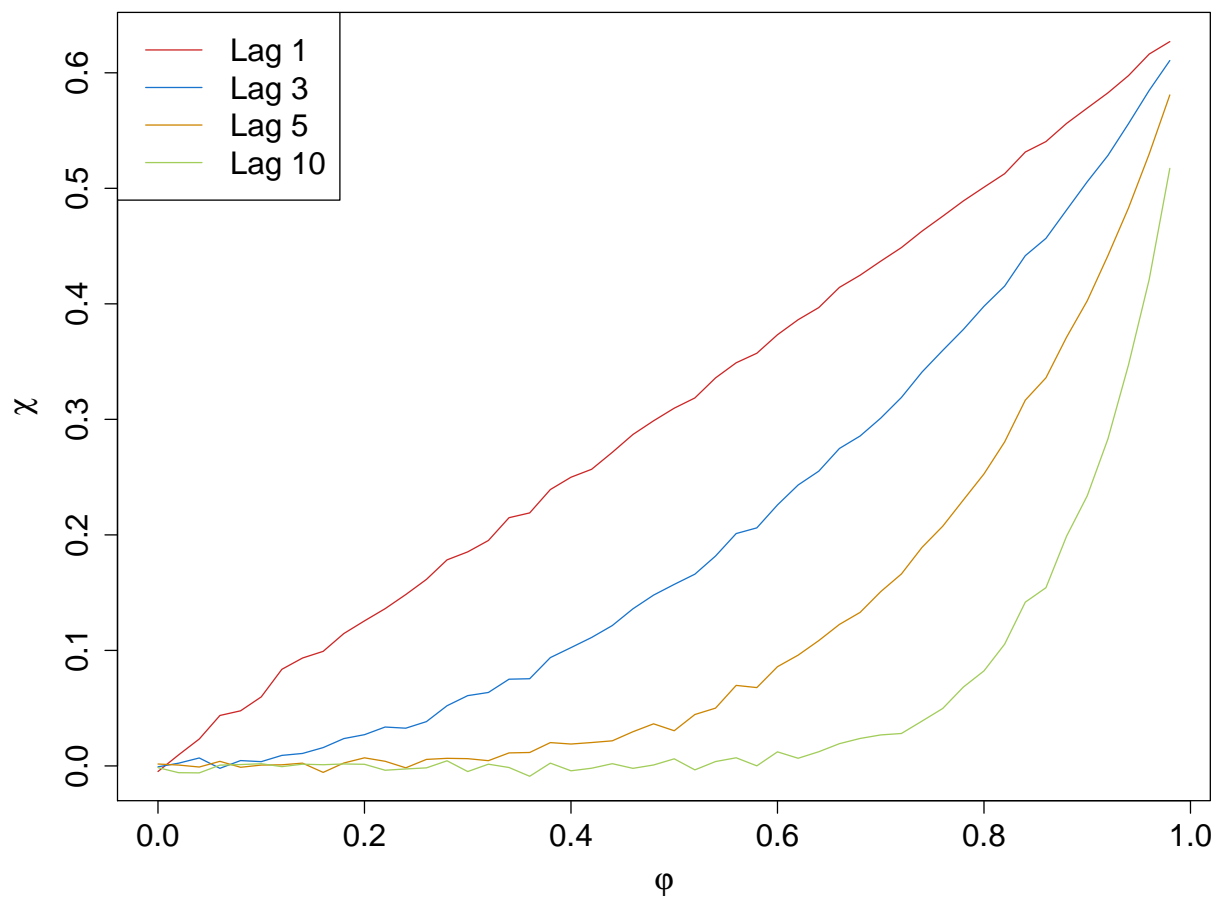
[Table 5 about here.]

## References

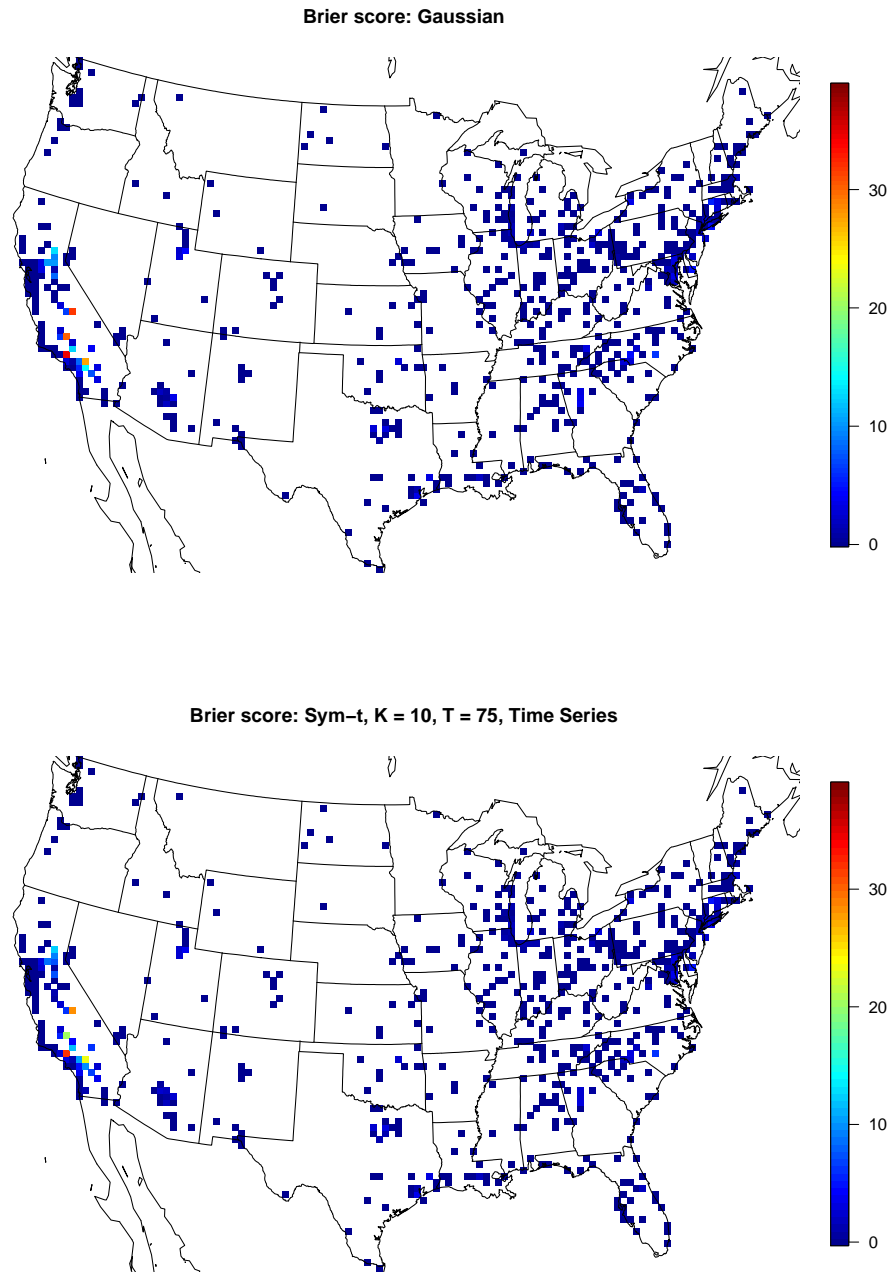
- Azzalini, A. and Capitanio, A. (2003). Distributions generated by perturbation of symmetry with emphasis on a multivariate skew t-distribution. *Journal of the Royal Statistical Society: Series B (Statistical Methodology)* **65**, 367–389.
- Azzalini, A. and Capitanio, A. (2014). *The Skew-Normal and Related Families*. Institute of Mathematical Statistics Monographs. Cambridge University Press.
- Beranger, B., Padoan, S. A., and Sisson, S. A. (2016). Models for extremal dependence derived from skew-symmetric families. *ArXiv e-prints*.
- Cooley, D., Naveau, P., and Poncet, P. (2006). Variograms for spatial max-stable random fields. In Bertail, P., Soulier, P., and Doukhan, P., editors, *Dependence in Probability and Statistics*, volume 187 of *Lecture Notes in Statistics*, chapter Variograms, pages 373–390. Springer New York, New York, NY.
- Padoan, S. A. (2011). Multivariate extreme models based on underlying skew- and skew-normal distributions. *Journal of Multivariate Analysis* **102**, 977–991.



**Web Figure 1.** Illustration of the partition of  $A$ .



**Web Figure 2.** Simulated lag- $m$   $\chi$  for varying levels of  $\phi$ .



**Web Figure 3.** Map of Brier scores for Gaussian (top) vs Symmetric- $t$ ,  $K = 10$  knots,  $T = 75$ , time series (bottom).

Web Table 1					
Setting 1 – Gaussian marginal, $K = 1$ knot					
	$q(0.90)$	$q(0.95)$	$q(0.98)$	$q(0.99)$	
Method 1	A	A	A	A	
Method 2	A	A	A	A	
Method 3	B	B	C	A	
Method 4	A	A	A B	A	
Method 5	B	B	B C	A	
Method 6	C	C	D	B	

**Web Table 2***Setting 2 – Skew-t marginal,  $K = 1$  knot*

	$q(0.90)$		$q(0.95)$		$q(0.98)$		$q(0.99)$	
Method 1	B		B		B		B	
Method 2	A		A		A		A	
Method 3	A	B	A	B	A	B	A	B
Method 4	A	B	A	B	A	B	A	B
Method 5	C		C		C		C	
Method 6	D		D		D		C	



Web Table 3

Setting 3 – Skew-*t* marginal, *K* = 5 knots

	<i>q</i> (0.90)	<i>q</i> (0.95)	<i>q</i> (0.98)	<i>q</i> (0.99)
Method 1	C	C	B	B
Method 2	C	C	B	B
Method 3	B	B	A	A
Method 4	A	A	A	A
Method 5	A	A	A	A
Method 6	D	D	C	C

**Web Table 4***Setting 4 – Max-stable, Asymmetric logistic*

	$q(0.90)$		$q(0.95)$		$q(0.98)$	$q(0.99)$	
Method 1	A	B		B	B		C
Method 2		B		B	B	B	C
Method 3			C	D	C	B	B
Method 4			D		D	C	C
Method 5			C		B	C	B
Method 6	A			A	A	A	

Web Table 5									
Setting 5 – Max-stable, Brown-Resnick									
			$q(0.90)$		$q(0.95)$		$q(0.98)$		$q(0.99)$
Method 1			D		C		C		C
Method 2			D		C		C		C
Method 3	A	B	A		A		B	B	
Method 4			C		B		B		B
Method 5	A		A		A		A		B
Method 6		B	C	A		A		A	